Seawater injection into reservoirs with ion exchange properties and high sulphate scaling tendencies: Modelling of reactions and implications for scale management, with specific application to the Gyda Field

R. A. McCartney (GeoScience Limited), K. Melvin, R. Wright (Talisman Energy UK Limited), E. Sørhaug (Talisman Energy Norge AS)

ABSTRACT

In part, the composition of produced water from fields under seawater flood is determined by reactions occurring in the reservoir. Understanding the nature and importance of these reactions can aid scale management during early development planning by ensuring that laboratory studies to select the most effective and efficient chemical inhibitors and predictions of scaling risk are more representative of reservoir conditions. Similarly, for producing fields, an understanding of these reservoir reactions can aid optimisation of chemical usage and squeeze treatment frequency.

Produced water analyses from well A-13 of the Gyda Field, Norwegian North Sea, are depleted in Mg, Ba and SO_4 relative to concentrations expected for seawater/formation water mixing. An earlier study by Mackay et al. (2006) used reactive transport modelling to show that such observations could be explained by barite and anhydrite deposition in the reservoir coupled with exchange of Ca from the formation for Mg in the seawater. In this study, further geochemical and reactive transport modelling has been undertaken to evaluate the role of multi-component ion exchange and dolomitisation in the reservoir, and to more fully investigate the relative role of factors influencing anhydrite deposition.

The results show that the reactions occurring in the reservoir are more complicated than at first thought with the depletion in Mg, Ba and SO_4 probably reflecting multi-component (Na, K, Ca, Mg) ion exchange, barite and calcite dissolution and precipitation, and anhydrite and brucite precipitation. Produced water compositions reflect these reactions and the seawater production profile for the well. There is a possibility that chlorite precipitation (perhaps at the expense of illite) and dolomitisation contribute to some Mg loss from the produced water. Further modelling studies are required to more fully evaluate the importance of these reactions and assess the importance of reaction kinetics. Other reactions may be occurring in the reservoir (e.g. plagioclase dissolution, K-feldspar dissolution) but do not significantly influence the produced water compositions.

The implications of this study with respect to qualitative predictions of future produced water compositions and scaling risks for Gyda wells are discussed. We also identify those factors determining anhydrite deposition in sandstone reservoirs, and comment on the benefits of geochemical and reactive transport modelling with respect to more representative scaling predictions and identification of conservative natural tracers.

INTRODUCTION

In reservoirs that are to be developed by seawater flood, deposition of mineral scale in oilfield production wells is a common risk. Scaling may be the result of production of formation water or formation water mixed with seawater. This risk must be assessed, and scale mitigation plans developed, during field appraisal and development, and subsequently managed during production. These activities are usually based on the assumption that the scaling risk will be determined by simple mixing of pure seawater and formation water in the production well. However, in the reservoir injected seawater reacts with both formation water and formation minerals so that the produced water composition usually does not correspond to a simple seawater/formation water mixture (Braden and McLelland, 1993; Mackay, 2003; Mackay and Jordan, 2003; Mackay et al., 2003; McCartney et al., 2005; Paulo et al., 2001; Petrovich and Hamouda, 1998; Sorbie and Mackay, 2000). There is an increasing trend of development of higher risk and cost projects (e.g. deepwater, marginal and subsea fields), so it is important to account for these reservoir reactions to obtain representative predictions of the scaling risk, to select the optimal scale mitigation strategy, and where necessary, to select the most effective and efficient chemical inhibitors. Similarly, for producing fields, an understanding of these reservoir reactions can aid optimisation of chemical usage and squeeze treatment frequency.

As an example of the benefits of understanding the reactions occurring in a reservoir under seawater flood, Mackay et al. (2006) recently evaluated those occurring in the Gyda field in the Norwegian North Sea. This is a mature, HTHP field containing formation water enriched in Ca, Ba and Sr. Mackay et al (op cited) noted that Ba, SO_4 and Mg were depleted in well A-20 produced water relative to mixed seawater/formation water and proposed that these ions were depleted as a result of barite and anhydrite deposition in the reservoir coupled with exchange of Ca from the formation for Mg in the seawater. Reactive transport modelling suggested that although anhydrite deposition can occur in this reservoir as a result of heating of injected seawater, and mixing of seawater and formation water, Ca released as a result of Mg-Ca ion exchange causes additional anhydrite deposition. The results of their study showed that scaling risks to the production wells were reduced because of these reservoir reactions such that MICs and inhibitor requirements in future may be lower than originally anticipated. Also, they noted that there is no sulphate scaling tendency until SO_4 breakthrough occurs (40-70% seawater). This tendency increases thereafter primarily as a result of anhydrite scaling risk at high seawater fractions. This contrasts with the more usual case where only barite deposition occurs and the scaling tendency decreases as seawater fractions increase above ~50%. They also suggested that the loss of Mg relative to Ca in the produced water may improve some inhibitor efficiencies and identified the potential impact of anhydrite precipitation near the injection well on injectivity.

Although the correlation of their modelling results with observed produced water analyses provides a compelling case, Mackay et al. (op cited) did not consider the role of other cations in the ion exchange mechanism and yet ion exchange is a competitive multi-component process (Appelo and Postma, 1999). Also, they did not discuss the relative importance of heating of seawater, mixing of seawater and formation water, and Ca-Mg exchange on anhydrite deposition and hence on the reduction of sulphate mineral scaling risk. Finally, they discounted dolomitisation as a process that might be occurring in the

reservoir on the grounds that the reaction is too slow. However, this mechanism of Mg removal has been proposed for other fields (Houston et al., 2006; Petrovich and Hamouda, 1998). In this paper, we report the results of further reactive transport modelling calculations that address these matters and we summarise the implications of our results to scale management on this and other similar fields.

BACKGROUND

Field and reservoir description

The Gyda field is located in Block 2/1 on the eastern flank of the Central Graben of the Norwegian Continental Shelf, approximately 270km southwest of Stavanger. It was discovered in 1980 and when production started in July 1990 it was the deepest, hottest and lowest permeability oilfield in the North Sea (Rothwell et al., 1993). The reservoir is located in Upper Jurassic shallow marine sands. Reservoir depth is 3650-4180mbsl and initial temperature and pressure were approximately 165^{o}C and 595 bar respectively. Three regions have been identified on the basis of PVT properties: the main field, south-west and Gyda South (Figure 1). The main field includes the crest and downdip areas and has a dip closure in the western parts called the C-sand area. The crest area has closure to the east by the Hidra fault system while it is stratigraphically-controlled to the south. Gyda South has a dip closure to the south-west and fault closure to the north-east. The reservoir has moderate to heavy faulting and pressure data indicate that the reservoir is compartmentalised.

A typical modal composition of the sandstone for Gyda South is shown in Table 1. Locally, detrital clay content (predominantly illite) can be variable (0-32%) and calcite cemented sandstones (hardgrounds) can also be present such that calcite has been seen to vary between 0 and 43 volume percent in thin section. Based on the mineralogical composition in Table 1 and using typical cation exchange capacities (CEC) for illite, chlorite and smectite (Appelo and Postma, 1999) the CEC of the Gyda South reservoir rock is estimated to be ~3.8 meq/100g (i.e. typical CEC for a sandstone with ~10% mica/clay content). Mean porosity for this area is 17%.

Gyda receives limited aquifer support and has been developed by seawater flood. Currently, there are 14 production wells and 9 injection wells across the field. Gyda formation water is Na-Ca-Cl brine, enriched in Ba and Sr. An example composition is given in Table 2 but the composition of the formation water is known to vary across the field. From the outset, it was recognised that produced water would have high scaling tendencies for carbonate and sulphate minerals and the current scale management strategy for all production wells is to squeeze them as son as they cut water and then continue to squeeze them every 1-2 years (Mackay et al., 2006).

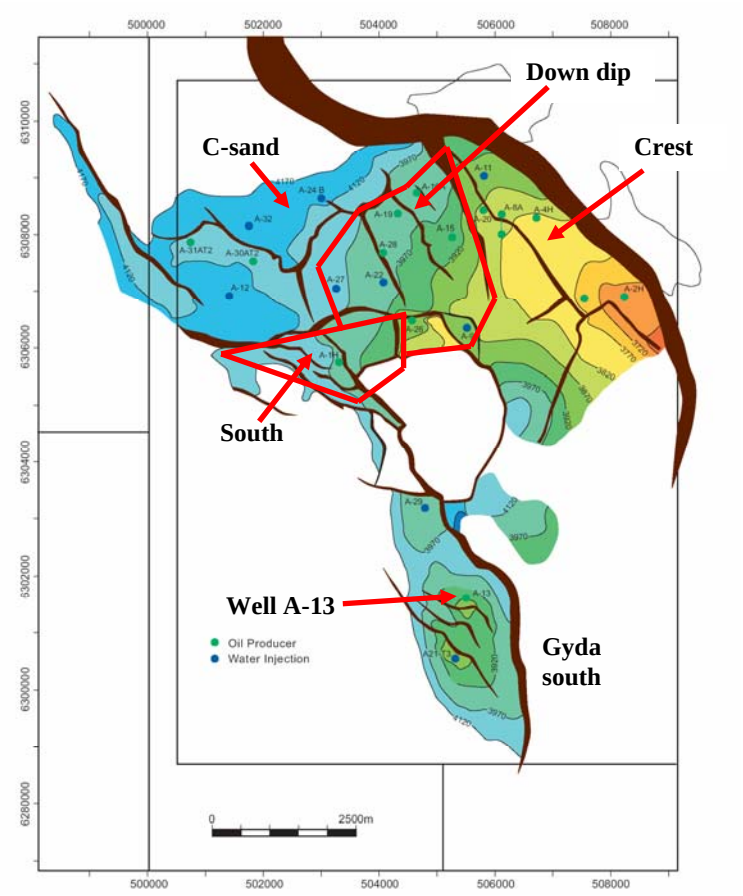

Figure 1 Gyda Field map showing well locations and major faults

Table 1 Typical mineralogical composition of reservoir sandstone in Gyda South

Mineral	Volume %
Quartz	60
K-feldspar	14
Plagioclase	9
Illite	8
Ferroan dolomite	4
Calcite	3
Chlorite	1
Smectite	1
Barite, siderite, pyrite, halite	<1

Produced water analyses

Produced water analyses act as an important constraint on the modelling of reservoir reactions. All Gyda production wells are currently producing water. One is only producing formation water but the rest are producing a mixture of seawater and formation water. Following a review of the produced water analyses it was concluded that the composition of formation water produced from individual wells in the crest area (including well A-20) is probably varying over time reflecting a variation in the areas of the reservoir from which formation water is being drawn. As this can complicate the interpretation of trends in produced water compositions, produced water analyses from well A-13 in the central part of Gyda South were selected for comparison with the model simulations. This is a high angle well, perforated between 3953m and 4056m TVDSS from which production started in August 1995. Water breakthrough occurred in October 2001 after which the water rate and cut increased within a few months to approximately 3500 bbls/day and 45% respectively. The water rate and cut have been variable about these values since this time. Pressure support for this well is provided by seawater injection in A-21 (injection started in September 1998) and/or A-29 (injection started in July 2000). For both injection wells, injection is into the oil-leg. Formation water produced from this well is believed to have maintained a consistent composition over time. The estimated formation water composition for this well is shown in Table 2, along with the composition of seawater used in this study. The Cl content of the formation water was assumed to be the same as that for adjacent well A-29 whilst the remaining composition was constrained by geochemical modelling (see below).

Table 2 Seawater and Gyda South A-13 formation water composition

Constituent	Seawater (mg/l)	Formation water (mg/l)
Na	10948	54560
K	406	6000
Mg	1313	1970[#]
Ca	418	36900
Sr	8	1290
Ba	0.01	1015
Cl	19700	162000
SO_4	2760	5
Total alkalinity*	151	197**
pH (reservoir)*	7.25	4.75**
Density	1.0232	1.1801

[#] 2040 mg/l Mg used in the dolomite model.

* 165^{o}C, 595 bar.

** Assuming equilibrium in the reservoir with Gyda South oil and calcite.

Produced water analyses for well A-13 are shown in Figures 2 and 3. Ion balances for these analyses are less than ±7% and uncertainties on the analyses are shown in Table 3. Seawater breakthrough, from A-21 and/or A-29 was marked by a rapid decline in Cl in produced water (Figure 3) and approximately coincided with the start of water production in this well suggesting that breakthrough occurred within the oil-leg. Figure 2 shows well A-13 produced water analyses against percentage seawater. The latter has been calculated assuming Cl is a conservative natural tracer. Produced water from well A-13 displays a wide range in seawater content (17-93%) and it can be seen that Na, K, Ca, and Sr lie along a simple mixing line between the formation water and seawater. This indicates that they are not significantly affected by reactions in the reservoir as a result of seawater injection. In contrast, Mg, Ba, and SO_4 lie below the mixing line indicating a net loss. Although produced water from this well is oversaturated with respect to barite (see below) it is not believed that significant Ba and SO_4 loss has occurred in the well or sample containers prior to analysis because produced water is protected by sulphate scale inhibitors and the trends in the analyses with varying seawater content are reasonably consistent. The net loss of each of these constituents is therefore likely to have occurred in the reservoir as a result of reaction.

Table 3 Uncertainty in produced water analyses arising from sampling and analysis. %RSD = relative standard deviation. Uncertainty for SO_4 is assumed.

Constituent	%RSD
Na	4.0
K	6.4
Mg	6.5
Ca	5.3
Sr	7.0
Ba	2.9
Cl	1.9
SO_4	10.0

Figure 3 shows well A-13 produced water analyses against time. Time 0 has been arbitrarily been selected to allow comparison with 1-D reactive transport modelling results (see below). A break in production occurred between April 2002 and November 2004 but this did not affect the trends in produced water compositions and this period has been removed from these figures. It can be seen that Na, K, Ca, Sr, and Cl display a gradual decline in concentration over time becoming fairly constant after approximately 800 days. Ba displays the same trend but is fairly constant after approximately 700 days. Mg declines up to approximately 750 days before increasing thereafter. SO_4 is low until approximately 600 days, increases to approximately 900 days and then declines to fairly constant concentrations after this time.

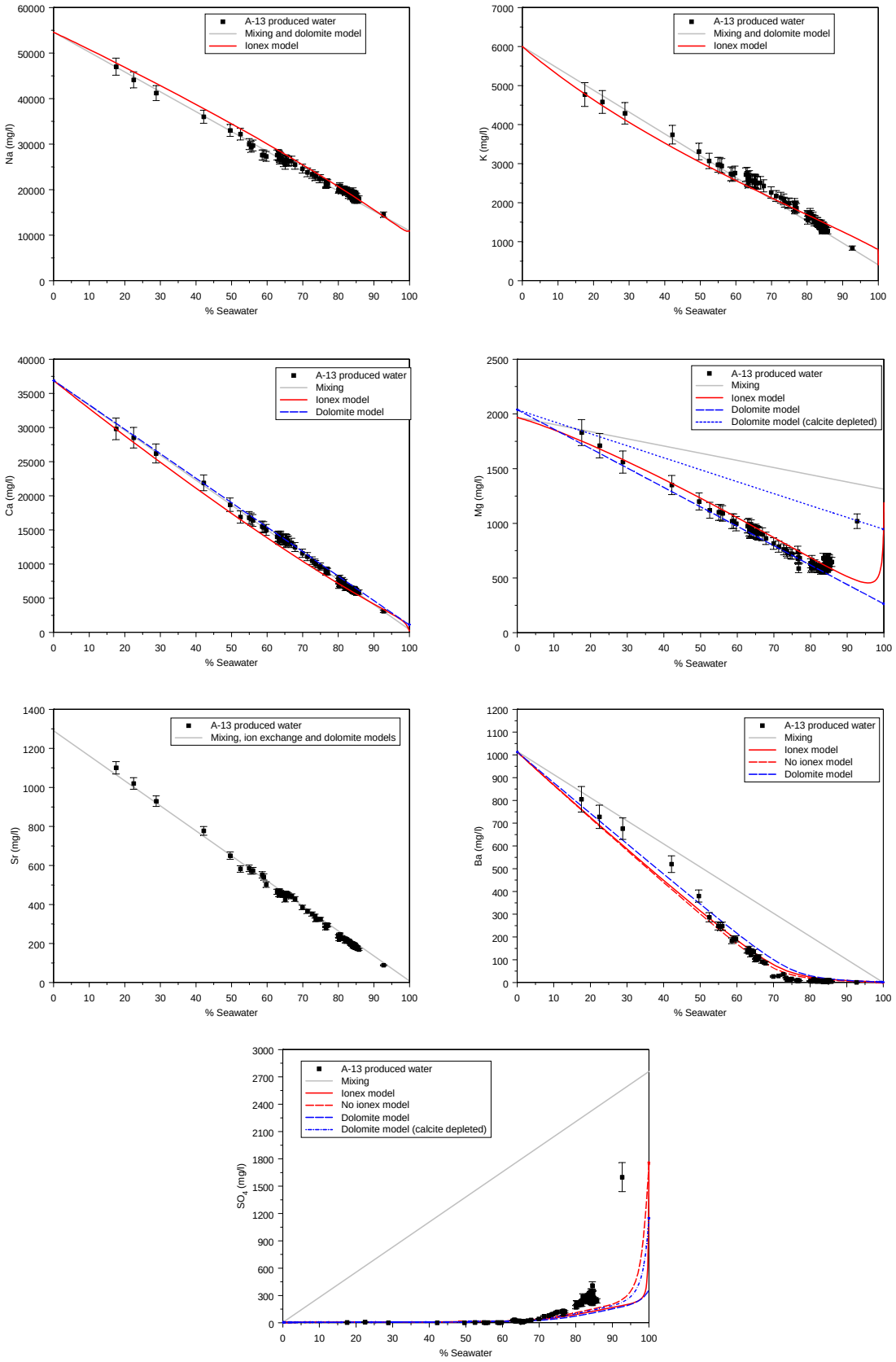

Figure 2 Produced water analyses and model simulation results against seawater content for Na, K, Ca, Mg, Sr, Ba, and SO_4.

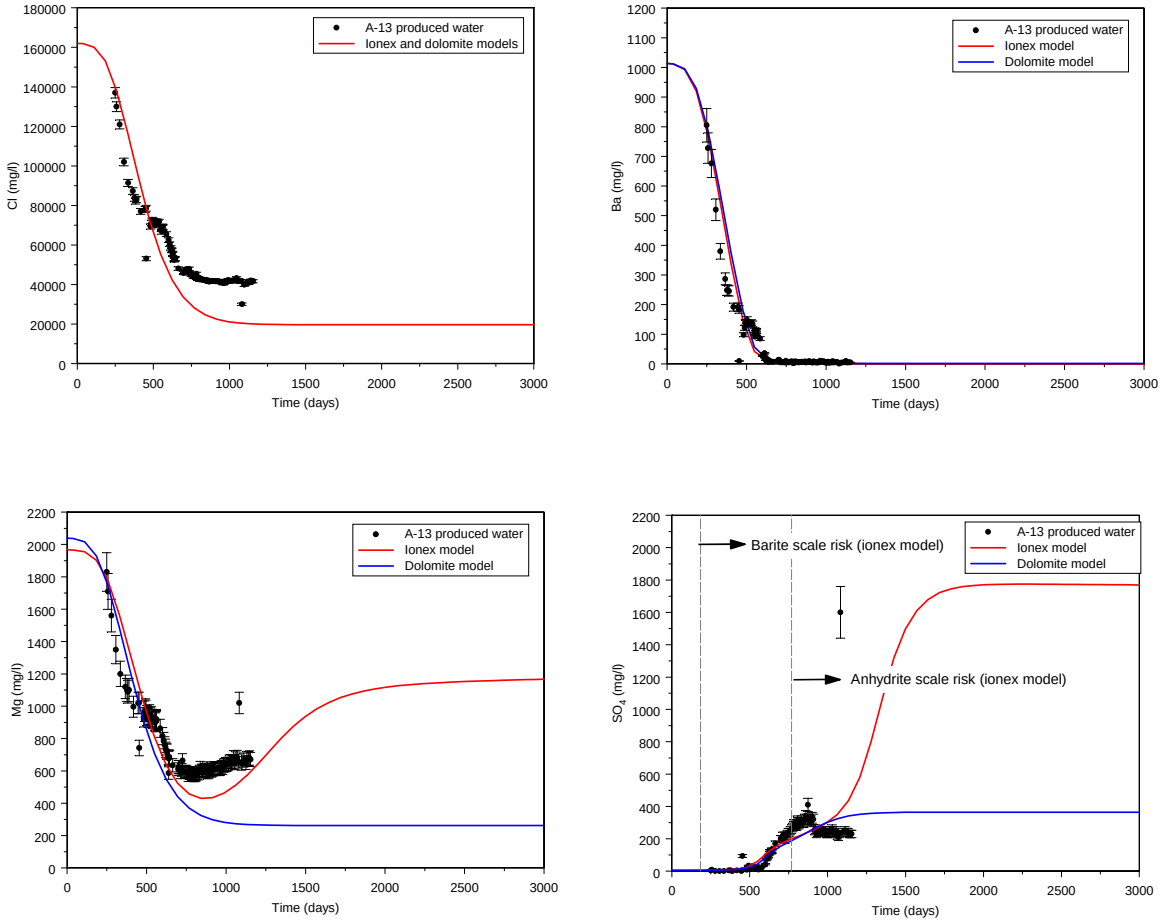

Figure 3 Produced water analyses and model simulation results against production time for Cl, Ba, Mg and SO_4.

GEOCHEMICAL AND REACTIVE TRANSPORT MODELLING

Reservoir reactions were modelled using Geochemist's Workbench (GWB) 6.04 (Bethke, 2005) using the Pitzer ion interaction parameters (H-Na-K-Mg-Ca-Sr-Ba-Fe-Cl-Br-HS-HSO_4-SO_4-HCO_3-CO_3-OH) and aqueous species equilibrium constants from MultiScale 7 (see Kaasa, 1998). Mineral solubility constants were taken from Kaasa (op cited) and SUPCRT92 (DSlop98.dat) (Johnson et al., 1991). Flash calculations were undertaken using GWB and MultiScale 7 (Petrotech, 2006) in a bench-marking exercise. These calculations simulated the mixing of seawater and well A-13 formation water at 165^{o}C and 595 bar pressure. Using MultiScale, seawater was heated to 165^{o}C and 595 bar before mixing. The reservoir composition of formation water was calculated at the same pressure and temperature assuming equilibrium with typical Gyda South oil (1.8 mole % CO_2) and calcite. The formation water and seawater compositions (constituent molalities) obtained from MultiScale were used in the flash calculations of both codes.

The saturation ratios and precipitated masses for various minerals obtained from the flash calculations were compared. It was found that the results of GWB did not produce

similar results to MultiScale because the former software does not include the pressure corrections to Pitzer parameters included in MultiScale. However, where GWB simulations were undertaken at 165^{o}C and 200 bars pressure, again using formation water and seawater compositions obtained from MultiScale at 165^{o}C and 595 bars pressure, the results were similar to those of MultiScale undertaken at 165^{o}C and 595 bars pressure (see Figure 2). Under these conditions, the lack of pressure correction of Pitzer parameters in GWB is compensated for by utilising aqueous species and mineral solubilities calculated at 200 bars pressure. To simulate reservoir conditions, reactive transport modelling was therefore performed using thermodynamic data obtained at 165^{o}C and 200 bars pressure and formation water and seawater compositions obtained from MultiScale at 165^{o}C and 595 bars pressure.

1-D reactive transport modelling was undertaken to simulate reactions occurring along a single flow path in the reservoir extending away from an injection well. The simulated reactions were constrained using produced water analyses and their associated seawater content (Figure 4). In addition to reproducing the produced water analyses, these simulations also helped constrain the formation water composition (see Table 2). Two models were found to approximately reproduce the observed trends in produced water compositions against seawater fraction. In each, seawater mixes with and displaces formation water from the flow path and similar reactions occur but in one ion exchange reactions are simulated (ion exchange model) and in the other dolomite precipitation is allowed (dolomite precipitation model; see Table 4). In both models, reactions are assumed to proceed sufficiently fast enough for equilibrium to be approximated. The ion exchange model is similar to the model proposed by Mackay et al. (2006) except that it allows multi-component ion exchange, barite dissolution, brucite precipitation, and calcite dissolution and precipitation.

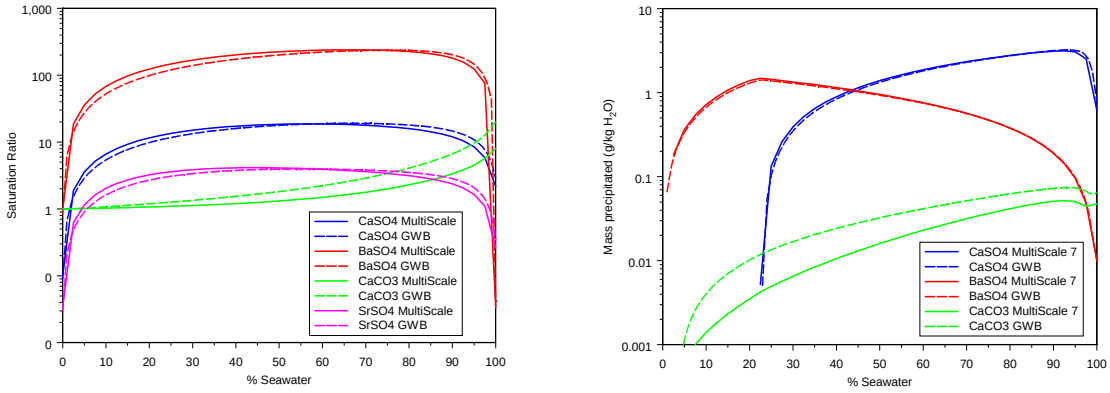

Figure 4 Comparison of saturation ratios and precipitated masses from flash calculations using MultiScale and Geochemist's Workbench

Table 4 Model conditions

Parameter	Ion exchange model	Dolomite model
Initial fluid	Formation water	Formation water
Injected fluid	Seawater	Seawater
Reactions	Ion exchange (Na, K, Ca, Mg) $K_{Na/K}$=0.2 $K_{Na/Mg}$=0.25 $K_{Na/Ca}$=0.2	
	Calcite, anhydrite, barite, brucite dissolution and precipitation*	Calcite, anhydrite, barite, Gyda dolomite dissolution and precipitation*
Host rock**	Calcite present	Calcite present
CEC of formation	3.8 meq/100g	
Path length	2500m	2500m
Nodes	100	100
Duration^	10 years[#]	10 years[#]
Porosity	0.17	0.17
Longitudinal dispersivity	20m	20m
Discharge rate	75 m yr^{-1}	75 m yr^{-1}
Diffusion coefficient	1 x 10^{-6} cm s^{-2}	1 x 10^{-6} cm s^{-2}

* These minerals can precipitate and re-dissolve later in the simulations if conditions allow.
** Calcite dissolves to equilibrium when fluids are undersaturated with respect to calcite.
[#] Data for Figure 3 are taken from entire path length after 1020 days flow. Data for Figure 6 are taken from position 1.066km along the path length.

In the ion exchange model, the Gaines-Thomas convention was used with selectivity coefficients taken from Appelo and Postma (1999). These are 'typical' selectivity coefficients for clays. Preliminary calculations indicated that seawater, formation water and mixtures of these were oversaturated with respect to ordered and disordered dolomite but in this model their precipitation was suppressed. Although allowing either to precipitate resulted in removal of Mg from seawater, Mg was also removed from the formation water producing Mg-deficient formation water compositions that are inconsistent with those observed in the Gyda field. By introducing a hypothetical disordered dolomite ('Gyda' dolomite) into the dolomite precipitation model, and fixing the solubility constant of this mineral to -0.15 (log K, 165°C, 200 bar, see Equation 1), it was possible to precipitate this mineral from seawater only (formation water and seawater/formation water mixtures were undersaturated with respect to Gyda dolomite) giving simulation results that were consistent with observed produced water analyses. The validity of each model is discussed more fully below.

$$CaMg(CO_3)_2(s) + 2H^+ \Leftrightarrow Ca^{2+} + Mg^{2+} + 2HCO_3^- \qquad \text{Eq. 1}$$

SIMULATION RESULTS

Ion exchange model

Figure 2 shows the produced water analyses and ion exchange model simulation results against seawater content for Na, K, Ca, Mg, Sr, Ba, and SO_4. It can be seen that generally there is a reasonable fit between the two data sets. The most notable discrepancies between the simulation and actual produced water analyses are enrichment in Mg above ~85% seawater and SO_4 above ~68% seawater, and depletion in Ba above ~68% seawater. These are discussed further below.

In detail, the reaction processes associated with our ion exchange model are more complicated that those previously proposed by Mackay et al. (op cited). As seawater is injected into an injection well and flows toward a production well, it mixes with and displaces formation water. In doing so, several sequential reaction zones are established. The dominant reactions occurring in each zone are identified in Table 5 and are shown in Figure 5.

Table 5 Principal reactions occurring along the flow path in the ion exchange model

Reaction zone	% Seawater*	Precipitation	Dissolution	Ion exchange
1	3.4-93.6	Barite	Calcite	Ca uptake, Na release
2	93.6-99.9	Anhydrite, calcite	Barite	Na, Mg uptake, Ca release
3	98.0-100	Anhydrite, calcite		Na, Mg uptake, K, Ca release
4	100	Calcite		Na, Mg uptake, K release
5	100			
6	100	Brucite, anhydrite	Barite, calcite	

* At time 1120 days.

Zone 6 remains located within the injection zone but the other reaction zones move away from the injection area over time, their positions relative to each other remaining the same. As a result, at any particular location along the path, which may be for example a production well, formation water will be initially observed (produced) followed by water associated with reaction zones 4, 3, 2 and 1 following injection water breakthrough. Table 5 also shows the seawater content of each zone at 1120 days to show how most of the reactions occur after almost all the formation water has been displaced. Barite deposition and calcite dissolution occur during displacement of the bulk of the formation water (Zone 1). The latter is induced by uptake of Ca from the mixed seawater/formation water on to the exchange surface (with consequent release of Na to solution). At locations where seawater flushes the last remnants of formation water from the flow path

(Zone 2), significant Ca is displaced from the exchange surfaces by Na and Mg from the seawater. This, along with mixing of formation water and seawater, causes anhydrite and calcite precipitation which in turn leads to dissolution of barite that was previously precipitated as the bulk of the seawater/formation water mixing zone was displaced. As further flushing with seawater occurs (Zone 3), both anhydrite and calcite continue to be precipitated but barite dissolution ceases due to the higher SO_4 content of the seawater. At this stage K and Ca are being displaced from the ion exchange surface by Na and Mg from the seawater. With further flushing (Zone 4), minor ion exchange reactions continue for awhile causing minor calcite precipitation. Finally, after sufficient flushing with seawater has occurred, the exchange surfaces in Zone 5 will be in equilibrium with seawater exiting the injection well area (Zone 6).

Seawater entering the reservoir (Zone 6) is undersaturated with respect to barite and oversaturated with respect to brucite, anhydrite and calcite at reservoir pressure and temperature. As a result, a minor amount of previously deposited barite formed during mixing of early injected seawater and formation water is dissolved to equilibrium raising Ba concentrations by ~0.35 mg/l. Deposition of anhydrite and brucite in this zone as a result of heating induces calcite dissolution (Eq. 2) with the net effect being a loss of ~995 mg/l SO_4, ~125 mg/l Mg, and ~200 mg/l Ca from the seawater. Seawater entering the reservoir might be more appropriately termed 'reacted' seawater.

$$2CaCO_3(s) + 2H_2O + Mg^{2+} + 2SO_4^{2-} \Rightarrow Mg(OH)_2(s) + 2CaSO_4(s) + 2HCO_3^- \qquad \text{Eq. 2}$$

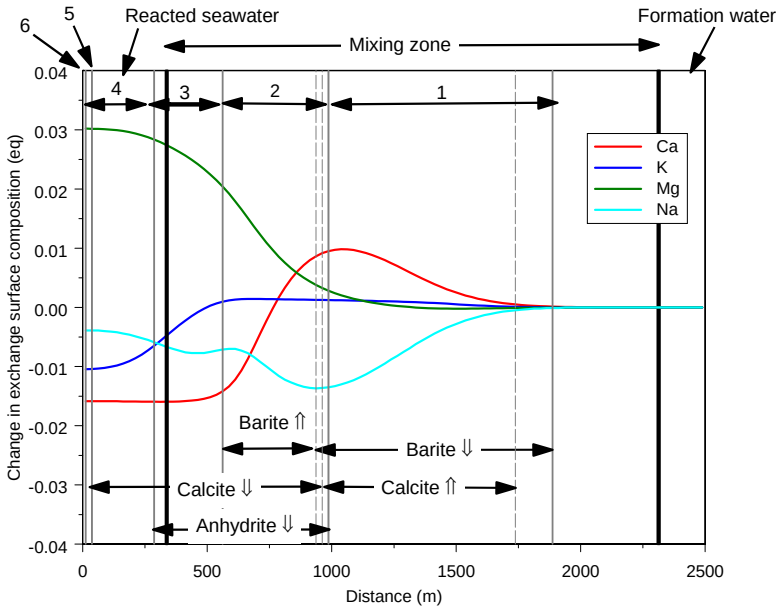

Figure 5 Change in ion exchange surface composition and mineral reactions occurring along the flow path after 1120 days. Injection zone = 0m distance.

Figure 6 shows the variation in Ba, SO_4 and Mg along the flow path. At Gyda relatively little Ba is lost from the mixed seawater and formation water relative to other fields where anhydrite precipitation does not occur (Mackay et al., 2006). It can be seen that this is because the formation water is mixing with SO_4-depleted seawater due to anhydrite deposition occurring in the injection well area and at the rear of the mixing zone. Likewise, the significant depletion in Mg at high seawater content (e.g. the front edge of Zone 2) is the result of mixing of formation water and Mg-depleted seawater due to loss of Mg from the injected seawater through brucite deposition near the injection well, and uptake of Mg on the exchange surfaces.

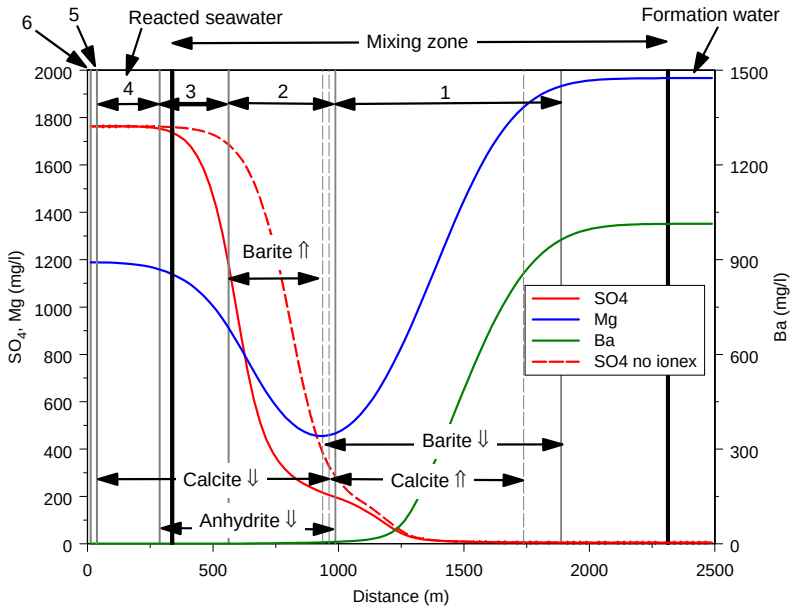

Figure 6 Ion exchange model: mineral reactions and variation of SO_4, Ba and Mg along the flow path after 1120 days. Injection zone = 0m distance.

Anhydrite is the dominant precipitate along the flow path but this and the ion exchange reactions have relatively little effect on Ca (i.e. in excess of analytical uncertainty) due to the high Ca concentrations in the fluids (see Figure 2). However, anhydrite precipitation does account for 92% of the loss of SO_4 from the water along the flow path. Based on the data presented in Figure 5, 36% of SO_4 is lost from seawater via heating induced anhydrite precipitation, approximately 56% is lost via anhydrite precipitation in Zones 2 and 3 and the remainder (~8%) is lost via barite precipitation and dilution by formation water in Zone 1. Interestingly, identical calculations undertaken without including ion exchange reactions indicate that only ~7% more SO_4 is lost as a by-product of ion exchange. Therefore, in order of importance for removal of SO_4 we have: mixing between reacted seawater and formation water > injection zone heating >> ion exchange effects. Presence or absence of ion exchange does not significantly modify the range of SO_4 concentrations in water along the flow path but does affect the spread of these data (see Figure 6). This is because when ion exchange occurs, release of Ca from exchange

surfaces allows anhydrite deposition to occur behind the seawater/formation water mixing zone.

Figure 3 shows well A-13 produced water analyses and model simulation results for a location 1 km from the injection zone against production time for Cl, Mg, Ba, and SO_4. Trends for Na, Ca, K, and Sr simulation results and produced water analyses are similar to those shown by Cl. The time axis for the model simulation results has been shifted to produce a reasonable fit with earlier produced water Cl analyses. This figure is not, therefore, intended to reproduce injection water breakthrough, but merely to allow direct comparison of observed and simulated trends in water compositions. It can be seen that there is a reasonable correlation between the trends over time shown by the model simulation and the produced water analyses. Exceptions are the late elevated Cl and Mg, and depleted SO_4 concentrations relative to the model results. We have simulated reactions along only one flow path but Sorbie and Mackay (2000) have noted that a variety of flow paths intersect a production well, each producing water with differing proportions of seawater and formation water at any one time. Under stable reservoir conditions, production from each flow path will change from formation water, through seawater/formation water mixtures to seawater. Given this conceptual model, the trend in well A-13 produced water Cl analyses reflects gradual seawater breakthrough into the well from a number of different flow paths. The cessation in decline of Cl after ~750 days probably reflects the onset of production of water with low seawater content (high Cl) from 'new' flow paths intersecting well A-13 at that time and thereafter. This interpretation also explains the cessation of increase in produced water SO_4 after 750 days. Late enrichment in Mg might be an effect of production of water with increasing seawater content from the flow paths where breakthrough occurred earlier (high seawater content, high Mg) although production of water from the secondary flow paths with higher formation water content (also high Mg) might also contribute to this effect. Additional calculations showed that Mg enrichment could also reflect production of water from flow paths with lower ion exchange capacity. These interpretations could also explain the trends in Mg and SO_4 in the produced water relative to the simulation results shown in Figure 2. Finally, the good fit between the simulated and produced water Ba analyses in Figure 3 is fortuitous, the low Ba during later production reflecting the low Ba content of the different waters being produced into the well from the different flow paths.

Dolomite precipitation model

The results of the dolomite precipitation model simulation were similar to those of the ion exchange model and so produced similar fits/discrepancies with respect to the produced water analyses (see Figures 2 and 3). The principal differences between the results of the two models are that in the dolomite model the reacted seawater contains much lower SO_4 (~370 mg/l SO_4) and Mg (~260 mg/l) and higher Ca (1120 mg/l). These differences reflect the reactions occurring in the injection well area. In the presence of calcite and seawater, heat-induced anhydrite precipitation and dolomite precipitation causes calcite dissolution and consumption of Mg and SO_4 moving reaction 3 (Eq. 3) to the right. This reaction proceeds until equilibrium is reached between the three solid phases leaving the seawater significantly depleted in Mg and SO_4. The higher Ca is produced from additional calcite dissolution associated with a reduction of pH in the reacted seawater. Minor barite dissolution also occurs.

$$2CaCO_3(s) + Mg^{2+} + SO_4^{2-} \Rightarrow MgCa(CO_3)_2(s) + CaSO_4(s) \quad \text{Eq. 3}$$

Again, as reacted seawater flows toward a production well, it mixes with and displaces formation water creating several reaction zones which, other than that around the injection area, move away from the injection well over time. The dominant reactions occurring in each zone along the flow path at 1120 days are identified in Table 6 and are shown in Figure 7. Barite deposition and calcite dissolution occur as a result of mixing during displacement of the bulk of the formation water (Zone 1). At locations where seawater flushes the last remnants of formation water from the flow path (Zone 2), mixing of formation water and seawater, causes anhydrite precipitation and calcite dissolution. Zone 3 contains reacted seawater which has exited from the injection well area (Zone 4).

Table 6 Reactions occurring along the flow path in the dolomite precipitation model

Reaction zone	% Seawater*	Precipitation	Dissolution
1	5.2-93.6	Barite	Calcite
2	93.6-99.9	Anhydrite	Calcite
3	99.9-100		
4	100	Anhydrite, dolomite	Calcite, barite

* At time 1120 days.

Figure 7 shows the variation in Ba, SO_4 and Mg along the flow path. As in the ion exchange model, because the formation water is mixing with SO_4-depleted seawater due to anhydrite deposition occurring in the injection well area less barite deposition occurs in the seawater/formation water mixing zone. Also, the apparent loss of Mg in the reservoir is due to mixing of formation water and Mg-depleted reacted seawater where loss of Mg has occurred through dolomite deposition near the injection well.

Anhydrite precipitation is again the principal cause of SO_4 removal from the water along the flow path. Based on the data presented in Figure 7, 87% of SO_4 is lost from seawater via injection zone reactions, a further 6% is lost via anhydrite precipitation in Zone 2 and the remainder (~7%) is lost via barite precipitation in Zone 1. The significantly higher amount of SO_4 loss associated with heating near the injection well is dependent on the amount of calcite present. If there is insufficient calcite present for the reaction to proceed to equilibrium, the SO_4 and Mg content of the reacted seawater will be higher on entering the reservoir (see Figure 7). This might occur where calcite is low initially, or where calcite has already been dolomitised by previous seawater injection (i.e. it has been consumed). In the extreme case where no calcite is present, dolomite does not precipitate but brucite and anhydrite do precipitate to equilibrium reducing SO_4 to 2130 mg/l and Mg only slightly below seawater values (1267 mg/l).

Figure 3 shows well A-13 produced water analyses and model simulation results for a location 1 km from the injection zone against production time for Cl, Mg, Ba, and SO_4.

Trends for Na, Ca, K, and Sr simulation results and produced water analyses are similar to those shown by Cl. The fits/discrepancies between the simulation results and the produced water analyses are similar to those identified in the ion exchange model except that the correlation with produced water SO_4 analyses appears improved whilst the reverse is true for Mg. Discrepancies between simulation and produced water Cl, Ba, Mg and SO_4 can be explained using similar arguments as those proposed for the ion exchange model. However, in this case, the late increase in Mg cannot be explained by increasing production of high seawater content water because this will have low Mg content. So, the late increase in Mg under this model may reflect production of low seawater content water (enriched in Mg) from 'new' flow paths. If these flow paths are also depleted in calcite, this may also help to raise the Mg content during late production.

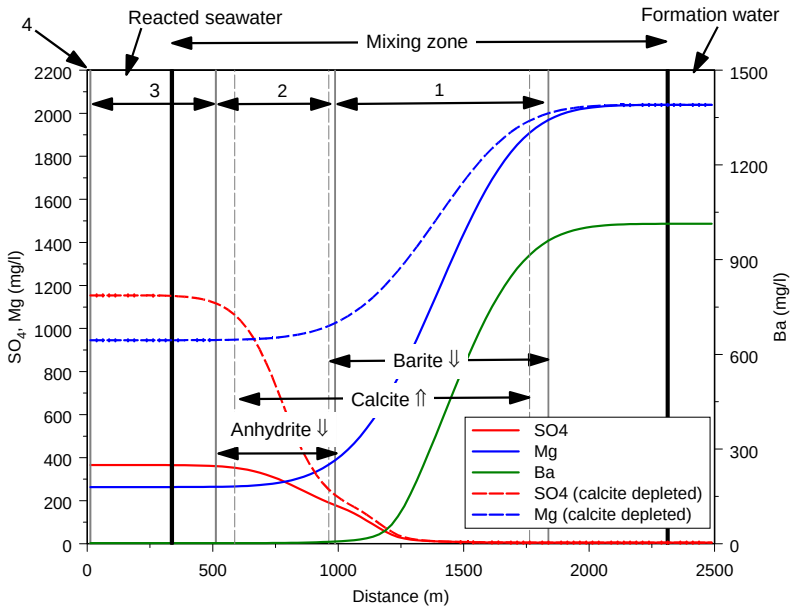

Figure 7 Dolomite precipitation model: mineral reactions and variation of SO_4, Ba and Mg along the flow path after 1120 days. Injection zone = 0m distance.

DISCUSSION

Which model is applicable to Gyda?

We have assumed equilibrium conditions in our ion exchange model calculations which is likely to be reasonable because ion exchange reactions are known to be rapid (milliseconds to hours) (Sposito, 1995) and preliminary calculations using estimated dissolution and precipitation rate constants (as appropriate) for barite, anhydrite and calcite suggest equilibrium for these minerals should be achieved within hours. We have also used acceptable estimates of CEC for the reservoir and ion exchange selectivity coefficients. Given that the ion exchange model results produced a reasonable match with the produced water analyses, and discrepancies between the data sets can be

explained, we conclude that multicomponent ion exchange reactions, brucite precipitation and maintenance of equilibrium with calcite, barite and anhydrite are likely to be occurring in the well A-13 area of the reservoir as a result of seawater injection.

Whether dolomitisation is also occurring is more speculative. Many produced water analyses from Gyda have higher SO_4 than observed in well A-13 (Figure 8). To explain these data it is necessary to assume that they have been derived from areas of the reservoir where less reaction with calcite has occurred. Also, preliminary calculations using estimated precipitation rate constants indicate that it is necessary to assume (a) nucleation of dolomite on ferroan dolomite, and (b) specific surface areas expected for fine-grained calcite and ferroan dolomite (5um crystal diameter) for equilibrium with calcite and Gyda dolomite to occur within ~100 days. We have needed to assume a high log solubility constant for Gyda dolomite (-0.15) relative to that derived from laboratory experiments for disordered dolomite (-0.73) and ordered dolomite (-1.59) (Johnson et al., 1991) and that for disordered dolomite estimated from Gulf of Mexico formation water analyses (log K = -0.90) (Hyeong and Capuano, 2001). We have also assumed that the use of 200 bar mineral solubility constants allow us to approximate reservoir conditions. Evidently, further work is required to establish whether these assumptions are reasonable. Therefore, at this stage we can only say that dolomite precipitation in the Gyda reservoir remains an outside possibility that might influence observed Mg and SO_4 concentrations in produced waters.

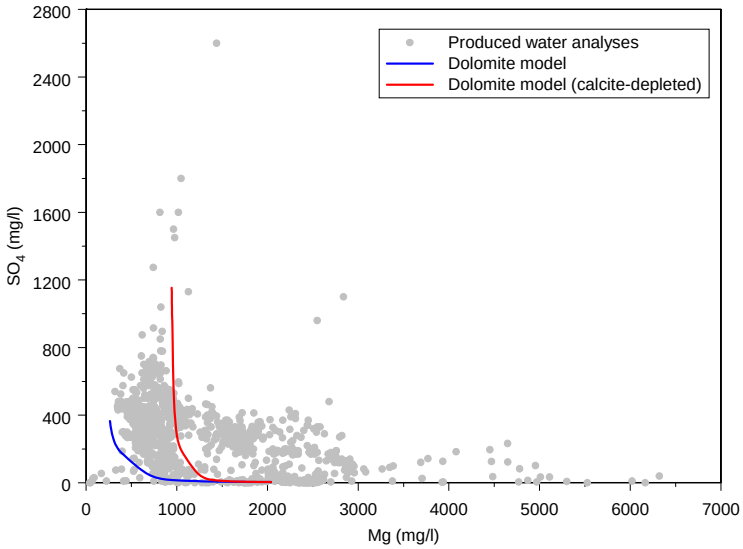

Figure 8 Produced water analyses (Mg, SO_4) for the Gyda field compared with results from the dolomite precipitation model (blue line = reaction to equilibrium with calcite, red line = reaction is a calcite depleted reservoir). The bulk of the high SO_4 analyses might be explained by the dolomite model by assuming less reaction with calcite. Samples enriched in Mg are believed to contain formation water that is enriched in Mg relative to well A-13 formation water and some may also be artifacts associated with analytical methods used during early production. A few high SO_4 samples have been obtained (>1200 mg/l SO_4) and these might possibly be contaminated with seawater during sampling.

Other reactions that might occur in the reservoir

Abundant sources of K (K-feldspar, illite), Na (plagioclase), and Ca (plagioclase) exist in the reservoir and there are also sources of Mg (chlorite, ferroan dolomite), Ba (barite), and Sr (calcite and plagioclase) but based on produced water compositions significant net release of these constituents during waterflood of Gyda South does not occur. Ferroan dolomite is likely to be stable with respect to seawater and formation water, but its stability with respect to mixed seawater/formation water is unknown. The anorthitic component of plagioclase is inherently unstable in oilfield environments, and albite and K-feldspar are unstable with respect to seawater, formation water and mixtures of these (see Figure 9). Some calcite and barite dissolution is predicted to occur in each model. Therefore, the lack of significant net gain of these constituents is probably due to lack of significant dissolution of these minerals rather than no reaction occurring at all. In any event, their reaction does not contribute significantly to the observed produced water compositions and at least for Na, K, Ca and Sr, the produced water composition is adequately described by simple seawater/formation water mixing.

Chlorite is present in the reservoir and the model compositions (and therefore produced water compositions) lie in the stability field of chlorite. This raises the possibility that precipitation of chlorite, perhaps at the expense of illite and/or K-feldspar, may contribute to the observed Mg loss. Unfortunately, Pitzer parameters for aluminium are not currently available and so these reactions cannot be modelled. The possibility of such reactions occurring therefore remains an uncertainty in this study.

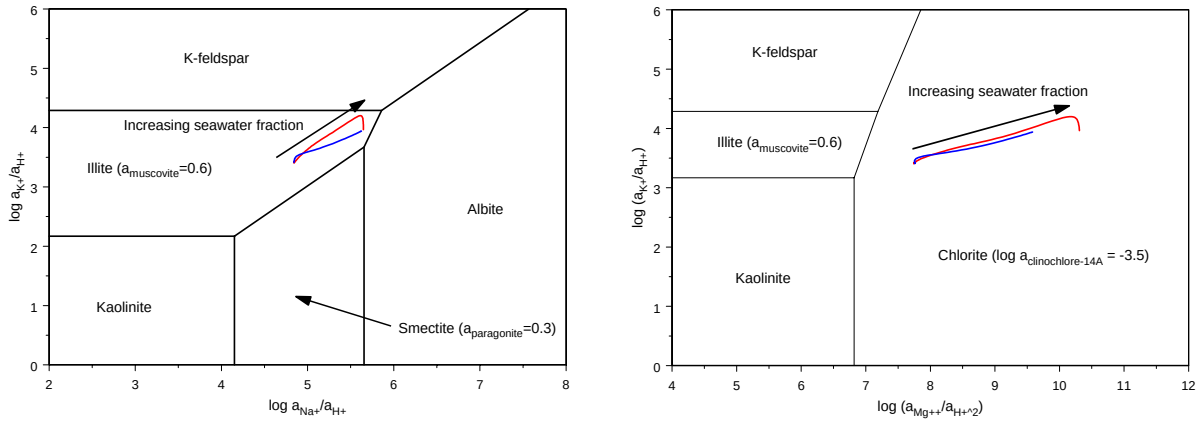

Figure 9 Stability diagrams for aluminosilicate minerals in the presence of quartz at 165°C and 200 bar pressure plotted versus (a) a_{K+}/a_{H+} and a_{Na+}/a_{H+} and (b) a_{K+}/a_{H+} and a_{Mg++}/a_{H+}^2 (thermodynamic data from Johnson et al., 1991). Water analyses for the ion exchange (red line) and dolomite precipitation (blue line) models are also shown.

IMPLICATIONS FOR SCALE MANAGEMENT

Qualitative predictions for Gyda wells

Mackay et al. (2006) have shown that reservoir reactions on the Gyda field can significantly reduce the sulphate mineral scaling risk, but the risk is not eliminated completely. To aid scale management on this field, it would be useful to be able to predict the future produced water compositions and scaling risk for different wells or field areas. Such information will aid (a) decisions on whether to reduce MICs and by how much, (b) estimations of future scale mitigation costs and (c) decisions regarding future changes in the types of chemicals used, should this be necessary. Quantitative predictions are possible using reservoir simulations (e.g. Daher et al., 2005) but even qualitative predictions can be useful. For example, for well A-13 we can generally expect the seawater production profile to increase giving reductions in produced water Na, K, Ca, Sr, Ba and Cl concentrations over time (Figure 3). Under the ion exchange model, Mg and SO_4 may continue increasing back toward reacted seawater concentrations ~1190 and ~1760 mg/l respectively. As Ba would be expected to remain low, the principal sulphate scaling risk in future will be from $CaSO_4$. There are, however, uncertainties in these predictions unrelated to the seawater fraction production profile. For example, the levels of Mg and SO_4 can be affected by the amount of clay minerals occurring along the different flow paths and dolomitisation might be occurring. It can be seen in Figure 3, that under the ion exchange model, the barite scale risk starts as soon as SO_4 starts to increase above formation water concentrations which for well A-13 was before the first water samples were collected whereas the anhydrite scaling risk starts later (~200 mg/l SO_4). This demonstrates that squeezing the well from first water cut was necessary but as discussed by Mackay et al. (2006) cost savings might be made in future by reducing MICs and decreasing squeeze treatment frequency.

More generally across the field, it may be possible to relate future produced water compositions to local geological conditions. For example, in areas where the sands are relatively clean, less ion exchange will occur so that produced water will be less Mg-depleted and Ca/Mg ratios will be lower. On the positive side, the duration of anhydrite scaling risk in these areas will be shorter, but on the negative side the efficiency of some inhibitors may be poorer. In contrast, the duration of anhydrite scaling risk will be more protracted in areas rich in argillaceous sands. Also, inhibitor efficiency may be improved temporarily (Mg concentrations will decrease but increase later in production as exchange site become saturated with Mg). If dolomitisation does occur, the effects on produced water compositions would be greatest in areas rich in calcite (e.g. where hardgrounds are present). In these areas, SO_4 and Mg can be maintained at lower levels in the produced water thereby reducing the sulphate scaling risk and increasing inhibitor efficiency (higher Ca/Mg). Previous studies (Mackay and Jordan, 2003) have noted how different reactions occurring in different types of reservoir (i.e. carbonate and sandstone reservoirs) can affect the scaling risk. Evidently, mineralogical variations within sandstone reservoirs may also be important.

Anhydrite deposition and its influence on produced water barite scaling risk

In both this study, and that of Mackay et al. (2006), it has been shown that at Gyda the barite scaling risk is reduced during earlier water production (lower seawater content) due to deposition of anhydrite in the reservoir. Anhydrite deposition is likely to occur in a number of circumstances in sandstone reservoirs under seawater flood:

1. Reservoir temperature >130^{o}C. Deposition can occur as a result of heating of seawater near the injection well and greater deposition will be associated with higher temperature reservoirs.

2. Presence of high Ca formation water. Deposition can occur as a result of mixing of seawater and formation water with greater deposition occurring in reservoirs with higher formation water Ca content and higher temperature (although this effect will be counteracted by greater deposition at higher temperature near the injection well).

3. Presence of argillaceous sands. The greater the clay content of the formation, the more anhydrite deposition will occur although in some fields, such as Gyda, this will be a secondary effect.

Evidently, based on these criteria, Gyda is an 'ideal' reservoir for anhydrite deposition. Anhydrite deposition might also occur with dolomitisation in some reservoirs. This is more likely to take place in calcite-bearing sands. Where this reaction does occur, more anhydrite will be deposited in higher temperature reservoirs with higher calcite content. Therefore, to understand factors influencing anhydrite deposition, it is important to understand the mechanism of Mg removal. Mg removal through ion exchange or dolomitisation promotes anhydrite deposition through release of Ca, whereas, for example, Mg removal via chlorite precipitation will not influence anhydrite deposition.

Initial scaling predictions

Although it is currently common practice to undertake 'conservative' scaling predictions involving formation water and seawater during early development planning for a field, this study has shown that the composition of seawater can undergo significant change in the reservoir directly related to heating and reaction with the formation and formation water. With the increasing development of higher risk projects, particularly when these are also higher temperature fields, there is a strong case for trying to determine the composition of reacted seawater that will mix with formation water and flow into the production wells during this planning stage so as to obtain more realistic scaling predictions. This might be achieved through a combination of laboratory (e.g. batch reactions of seawater and core, core floods, etc) and geochemical modelling studies.

Conservative natural tracers

In some fields, squeeze treatments will be delayed until injection water breakthrough is confirmed and thereafter MICs will be determined based on the seawater fraction in produced water. Both identification of breakthrough and calculation of the seawater fraction require the use of seawater and formation water analyses of conservative natural

tracers. These are constituents that are defined as 'not being significantly affected by reactions in the reservoir during waterflood'. Commonly Cl is used as a conservative natural tracer but this is of less use when formation water and injected water Cl compositions are similar or where halite is present in the reservoir. Also, where formation water compositions vary across the reservoir sometimes changes in produced water compositions can be the result of production of varying fractions of different formation waters. In these circumstances it is necessary to make use of at least two conservative natural tracers to discriminate between this scenario and injection water breakthrough. A further benefit of undertaking seawater reaction studies is that those constituents that are not significantly affected by reaction can be identified. These have the potential to be conservative natural tracers. At Gyda, at least in the A-13 area, Na, K, Ca, Sr and Cl are all conservative natural tracers.

CONCLUSIONS

Geochemical and reactive transport modelling of reactions between seawater, formation water and the formation in the well A-13 area of the Gyda Field have shown that produced water compositions reflect both reactions in the reservoir (probably multi-component ion exchange, barite and calcite dissolution and precipitation, and anhydrite and brucite precipitation) and the seawater production profile for the well. These results largely consistent with those of an earlier study by Mackay et al. (2006) although the reaction mechanism is more complicated than they originally proposed.

There is a possibility that chlorite precipitation (perhaps at the expense of illite and/or K-feldspar) and dolomitisation contribute to some Mg loss from the produced water. Further modelling studies are required to more fully evaluate the importance of these reactions and assess the importance of reaction kinetics. Other reactions may be occurring in the reservoir (e.g. plagioclase dissolution, K-feldspar dissolution) but do not significantly influence the produced water compositions.

More generally, this study has shown that in sandstone reservoirs under seawater flood:

1. Anhydrite deposition in the reservoir can significantly reduce the sulphate mineral scaling risk.

2. Anhydrite deposition can be expected in high temperature reservoirs and/or those containing high Ca content formation water (e.g. Clyde, Fulmar, Skua, and Heron fields in the UK North Sea). Ion exchange and dolomitisation reactions (i.e. the mechanism of Mg removal) between the formation and seawater and seawater/formation water mixtures can also influence the amount of anhydrite deposited in the reservoir.

3. Variations in the mineralogical composition across a reservoir may influence scale management.

Finally, we have demonstrated that, along with laboratory studies, geochemical and reactive transport modelling can make a useful contribution to the understanding of reactions occurring in the reservoir. This information can benefit scale management in

terms of providing more realistic scaling predictions during early development planning, providing qualitative predictions of trends in future produced water compositions and scaling risk for different wells across the reservoir, and identifying potential conservative natural tracers.

ACKNOWLEDGEMENTS

The authors thank the management of Talisman Energy (UK) Limited, Talisman Energy Norge AS and GeoScience Limited for permission to publish this paper.

REFERENCES

Appelo, C. A. J., and D. Postma, 1999, Geochemistry, Groundwater and Pollution: Rotterdam, A. A. Balkema, 536 p.

Bethke, C. M., 2005, The Geochemist's Workbench User Guide (Release 6.0), Hydrogeology Program, University of Illinois.

Braden, J. C., and W. G. McLelland, 1993, Produced water chemistry points to damage mechanisms associated with seawater injection: SPE Western Regional Meeting, p. 167-178.

Daher, J. S., J. A. T. Gomes, F. F. Rosario, M. C. M. Bezerra, E. J. Mackay, and K. S. Sorbie, 2005, Evaluation of inorganic scale deposition in an unconsolidated reservoir by numerical simulation: SPE 7th International Symposium on Oilfield Scale.

Houston, S. J., B. W. D. Yardley, P. C. Smalley, and I. R. Collins, 2006, Precipitation and dissolution of minerals during waterflooding of a North Sea oil field: International Oilfield Scale Symposium.

Hyeong, K., and R. M. Capuano, 2001, Ca/Mg of brines in Miocene/Oligocene clastic sediments of the Texas Gulf Coast: Buffering by calcite/disordered dolomite equilibria: Geochimica et Cosmochimica Acta, v. 65, p. 3065-3080.

Johnson, J. W., E. H. Oelkers, and H. C. Helgeson, 1991, SUPCRT92: A software package for calculating the standard molal thermodynamic properties of minerals, gases, aqueous species, and reactions from 1 to 5000 bars and 0 to 1000^{o}C, Laboratory of Theoretical Geochemistry, University of California, Berkeley, p. 114.

Kaasa, B., 1998, Prediction of pH, mineral precipitation and multiphase equilibria during oil recovery: IUK-Thesis: 89 thesis, The Norwegian University of Science and Technology, 7491 Trondheim, Norway.

Mackay, E. J., 2003, Modelling in-situ scale deposition: The impact of reservoir and well geometries and kinetic reaction rates: SPE Production and Facilities, p. 45-56.

Mackay, E. J., and M. M. Jordan, 2003, Natural sulphate ion stripping during seawater flooding in chalk reservoirs: Chemistry in the oilfield VIII.

Mackay, E. J., M. M. Jordan, and F. Torabi, 2003, Predicting brine mixing deep within the reservoir and its impact on scale control in marginal and deepwater developments: SPE Production and Facilities, p. 210-220.

Mackay, E. J., K. S. Sorbie, V. Kavle, E. Sørhaug, K. Melvin, K. Sjursæther, and M. M. Jordan, 2006, Impact of in-situ sulphate stripping on scale management in the Gyda Field: SPE 8th International Symposium on Oilfield Scale.

McCartney, R. A., J. C. Williams, and G. Coghlan, 2005, Processes determining the composition of produced water from subsea fields and implications for scale management - Birch Field, UKCS: SPE 7th International Symposium on Oilfield Scale.

Paulo, J., E. J. Mackay, N. Menzies, and N. Poynton, 2001, Implications of brine mixing in the reservoir for scale management in the Alba Field: SPE International symposium on oilfield scale.

Petrotech, 2006, MultiScale Version 7 User Manual: Haugesund, Norway.

Petrovich, R., and A. A. Hamouda, 1998, Dolomitisation of Ekofisk oilfield reservoir chalk by injected seawater: Proceedings of the 9th International Symposium on Water- Rock Interaction, p. 345-348.

Rothwell, N. R., A. Sørensen, J. L. Peak, K. Byskov, and T. A. M. McKean, 1993, Gyda: Recovery of difficult reserves by flexible development and conventional reservoir management: SPE European IOR Symposium.

Sorbie, K. S., and E. J. Mackay, 2000, Mixing of injected, connate and aquifer brines in waterflooding and its relevance to oilfield scaling: Journal of Petroleum Science and Engineering, v. 27, p. 85-106.

Sposito, D. L., 1995, Environmental soil chemistry, Academic Press, U.S.A.